New Silver (Thio)Semicarbazide Derivatives: Synthesis, Structural Features, and Antimicrobial Activity†

Tiago A. Fernandes,[a,b] Vânia André,[a] Aliaksandr S. Arol,[a,c] Ângela França,[d] Sergei Mikhalyonok,[c] Nuno Cerca[d,*] and Alexander M. Kirillov[a,e,*]

[a]*Centro de Química Estrutural and Departamento de Engenharia Química, Instituto Superior Técnico, Universidade de Lisboa, Av. Rovisco Pais, 1049-001 Lisboa, Portugal; kirillov@tecnico.ulisboa.pt*
[b]*Departamento de Química e Bioquímica, Faculdade de Ciências, Universidade de Lisboa, Campo Grande, 1749-016 Lisboa, Portugal*
[c]*Department of Organic Chemistry, Belarusian State Technological University, 13a Sverdlova St., 220006 Minsk, Belarus*
[d]*Centre of Biological Engineering, University of Minho, Campus de Gualtar, 4710-057 Braga, Portugal; nunocerca@ceb.uminho.pt*
[e]*Research Institute of Chemistry, Peoples' Friendship University of Russia (RUDN University), 6 Miklukho-Maklaya st., Moscow, 117198, Russian Federation*

Electronic Supplementary Information (ESI)

†Electronic Supplementary Information (ESI) contains: data on single-crystal X-ray diffraction (Table S1) and additional structural representations (Figs. S1, S2); FT-IR (Figs. S3−S6), NMR (Figs. S7−S21), and ESI-MS (Figs. S22, S23) data.

Single Crystal X-ray Diffraction. Single crystals of compounds **1**−**4** suitable for X-ray diffraction were mounted with Fomblin© in a cryoloop. Diffraction data were collected on Bruker AXS-KAPPA APEX II or BRUKER D8 QUEST diffractometers (graphite-monochromated radiation, Mo Kα, λ = 0.7107 Å). X-ray generator parameters were 50 kV and 30 mA. Data for **1**−**3** were collected at 293 K; for **4** at 150 K. APEX2 and APEX3 programs were used to monitor the collection of X-ray data. SAINT and SADABS were applied for correction of all data for Lorentzian, polarization, and absorption effects. SHELXT 2014/4[S1] was used for structure solution, while SHELXL 2014/7 was applied for full matrix least-squares refinement on F^2.[S2] These programs are included in the package of programs, WINGX-Version 2014.1.[S3] Non-hydrogen atoms were refined anisotropically. A full-matrix least-squares refinement was used for the non-hydrogen atoms with anisotropic thermal parameters. All the hydrogen atoms bonded to carbon atoms were inserted in idealized positions and allowed to refine in the parent carbon atom. Hydrogen atoms connected to nitrogen atoms were located from the electron density map. A disorder model was used in one of the phenyl rings of **2**, with occupancies of 0.3:0.7

(values fixed after refinement). The crystal structures **1**−**3** have been deposited at the Cambridge Structural Database (CCDC numbers 1982198-1982200).

Despite the multiple attempts to collect data (ca. 10 datasets for different single crystals were collected) and the use of low temperature (150 K), the very sparse crystal diffraction of crystals of **4** and the limited time before radiation damage, leading to a total absence of diffraction, precluded the acquisition of good quality data (low ratio of observed/unique reflections (21%)) to achieve a stable refinement; AFIX66 instruction was used for the aromatic rings; the NO_2 groups have been identified but their refinement is unstable. Despite the low quality, a brief discussion of the structure of **4** was included due its relevance to confirm the Ag_6 core, which was unambiguously established. The CIF file of **4** was not deposited within CCDC but is available as ESI.

For topological analysis of H-bonded networks, a concept of the underlying net was applied.[S4,S5] Such simplified nets were generated by contracting discrete organic or metal-complex units to the respective centroids, preserving their connectivity. Only strong hydrogen bonds (D–H···A) were taken into consideration, with the following parameters: D···A <3.50 Å, H···A <2.50 Å, and ∠(D–H···A) >120°; D/A refer to donor/acceptor atoms.

Supplementary references

S1. Sheldrick, G. M., SHELXT - Integrated space-group and crystal-structure determination. Acta Crystallographica a-Foundation and Advances 2015, 71, 3-8.

S2. Sheldrick, G. M., Crystal structure refinement with SHELXL. Acta Crystallographica Section C-Structural Chemistry 2015, 71, 3-8.

S3. L.J. Farrugia, WinGX - Version 1.80.05. *J. Appl. Cryst.* 1999, **32**, 837–838.

S4. V.A. Blatov, *IUCrCompComm Newsletter*, 2006, **7**, 4–38.

S5. V.A. Blatov, A.P. Shevchenko and D.M. Proserpio, *Cryst. Growth Des.*, 2014, **14**, 3576–3586.

S6. M. Monroe, Molecular Weight Calculator Version 6.50 (Build 246) November 21, 2014.

Table S1. Crystal Data and Structure Refinement Details for **1**−**4**.

	1, HL[1]	**2**, HL[2]	**3**	**4**[c]
Formula	$C_{14}H_{12}N_4O_3$	$C_{14}H_{12}N_4O_2S$	$C_{14}H_{14}AgN_5O_7$	$C_{84}H_{53}Ag_6N_{24}O_{12}S_6$
Fw	284.28	300.34	472	2430.09
Crystal form, color	Block, colourless	Block, yellowish	Plate, brownish	Plate, orange
Crystal size (mm)	0.30×0.30×0.10	0.18×0.08×0.04	0.20×0.10×0.06	0.08×0.03×0.02
Crystal system	Monoclinic	Monoclinic	Triclinic	Triclinic
Space group	$P2_1/c$	$P2_1/c$	P-1	P-1
a, Å	15.5740(15)	9.187(3)	8.968(3)	13.787(3)
b, Å	10.7264(11)	34.222(10)	9.327(4)	16.498(3)
c, Å	8.1105(8)	4.7335(14)	11.613(4)	26.322(5)
α, deg	90.00	90.00	95.389(16)	77.056(9)
β, deg	96.563(5)	107.932(8)	95.673(16)	84.558(9)
γ, deg	90.00	90.00	104.311(16)	69.367(7)
Z	4	4	2	2
V, Å^3	1346.0(2)	1415.9(7)	929.6(6)	5460(2)
T, K	293(2)	293(2)	293(2)	150(2)
D_c, g cm^{-3}	1.403	1.409	1.687	1.478
μ(Mo Kα), mm^{-1}	0.102	0.238	1.131	1.231
θ range (°)	3.162–26.438	2.936–26.510	2.771–26.664	1.347–26.618
refl. collected	17544	9969	10962	49269
independent refl.	1964	1432	3818	22212
R_{int}	0.0561	0.0677	0.0492	0.1604
R_1 [a], wR_2 [b] [$I \geq 2\sigma(I)$]	0.0406, 0.1006	0.0572, 0.1255	0.0397, 0.1012	0.0994, 0.2205
GOF on F^2	1.038	1.012	1.059	0.803

[a] $R_1 = \Sigma||F_o| - |F_c||/\Sigma|F_o|$. [b] $wR_2 = [\Sigma[w(F_o^2 - F_c^2)^2]/\Sigma[w(F_o^2)^2]]^{1/2}$. [c]Despite a low quality, a brief discussion of structure of **4** was included due its relevance to confirm the Ag_6 core. The CIF file of **4** was not deposited within CCDC but is available as ESI.

(a) (b)

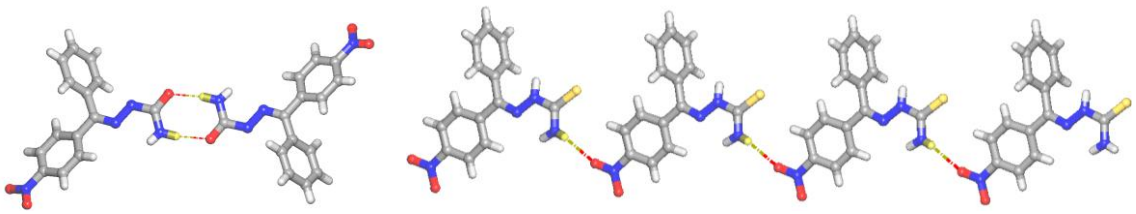

Figure S1. Structural fragments of **1** (a) and **2** (b) showing the formation of H-bonded dimers and 1D chains, respectively. Color codes: C (gray), H (white), N (blue), O (red), S (yellow), H bonds are shown as dotted lines (H atoms involved in hydrogen bonds are represented in yellow).

(a) (b)

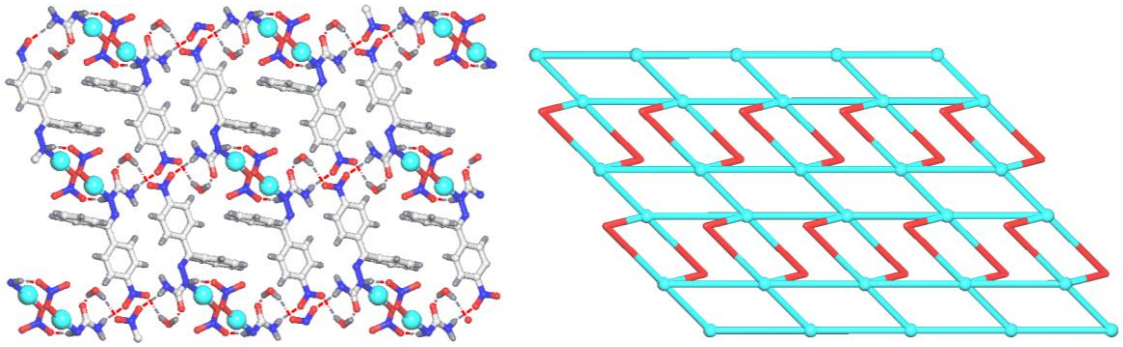

Figure S2. Structural fragments of **3**. (a) 2D H-bonded layer. (b) Topological representation of a simplified underlying 2D layer with the **sql** topology. (a) Color codes: Ag (cyan), C (pale gray), H (gray), N (blue), O (red), H bonds are shown as dotted lines. (b) Centroids of $[Ag(HL^1)(NO_3)]$ nodes (cyan balls), H_2O linkers (red).

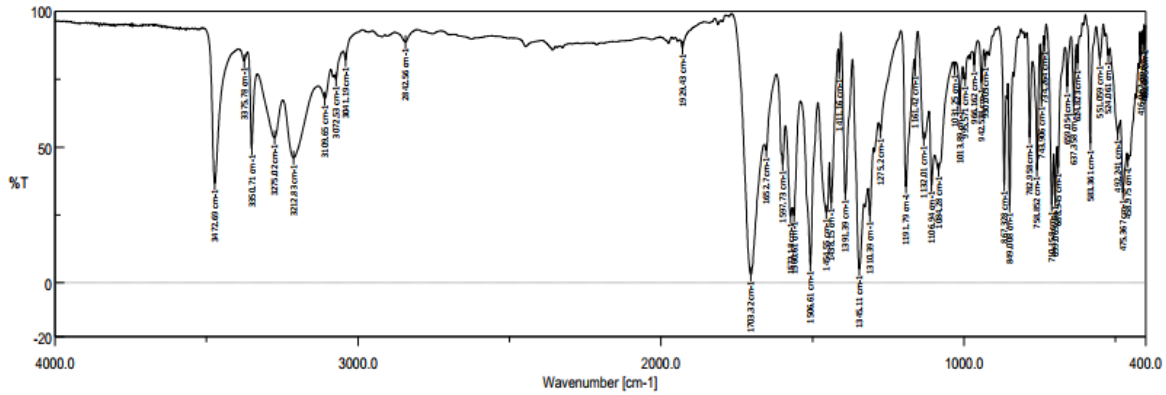

Figure S3. FTIR spectrum of compound **1**.

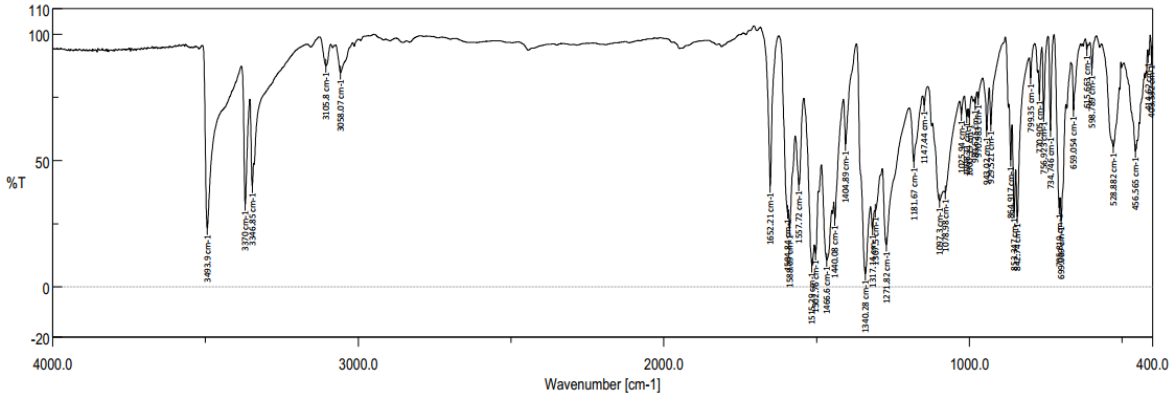

Figure S4. FTIR spectrum of compound **2**.

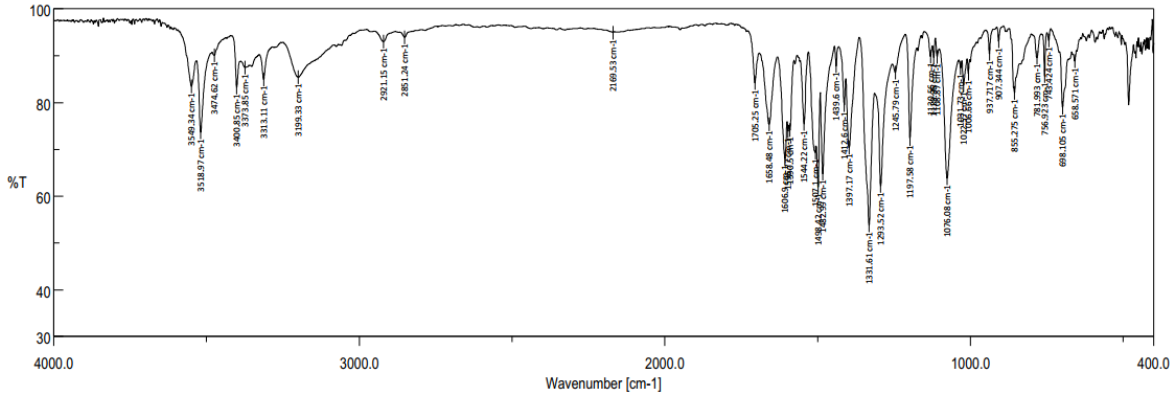

Figure S5. FTIR spectrum of compound **3**.

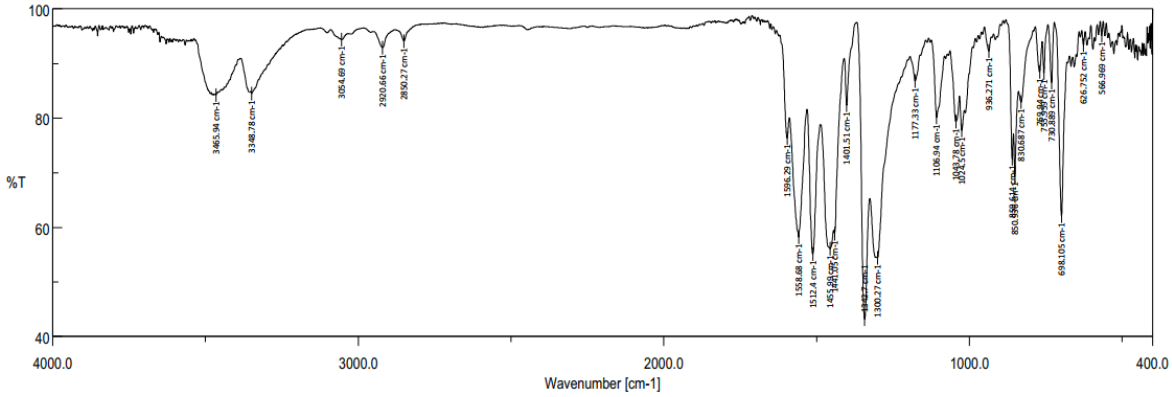

Figure S6. FTIR spectrum of compound **4**.

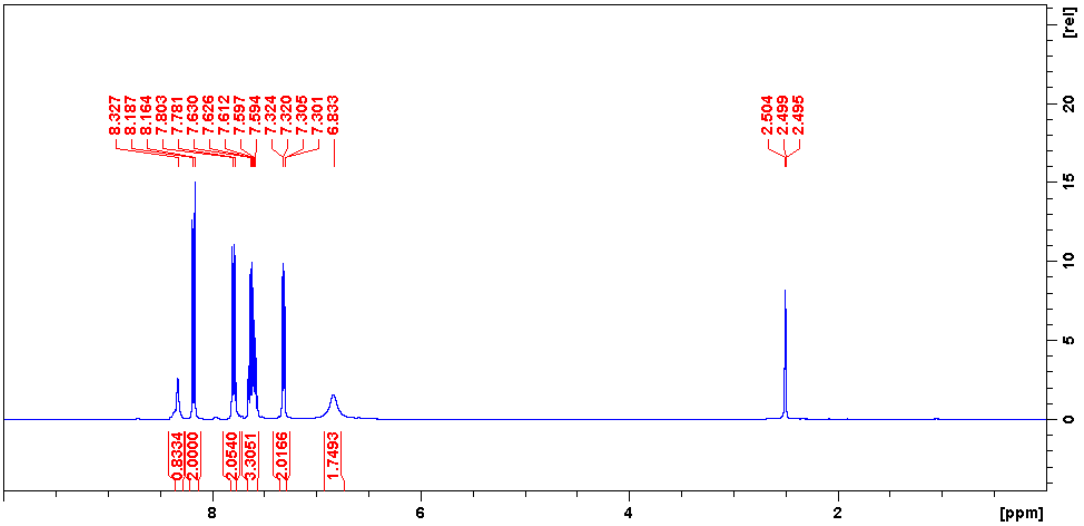

Figure S7. ^{1}H NMR spectrum of compound **1** (DMSO-d_6, 400 MHz).

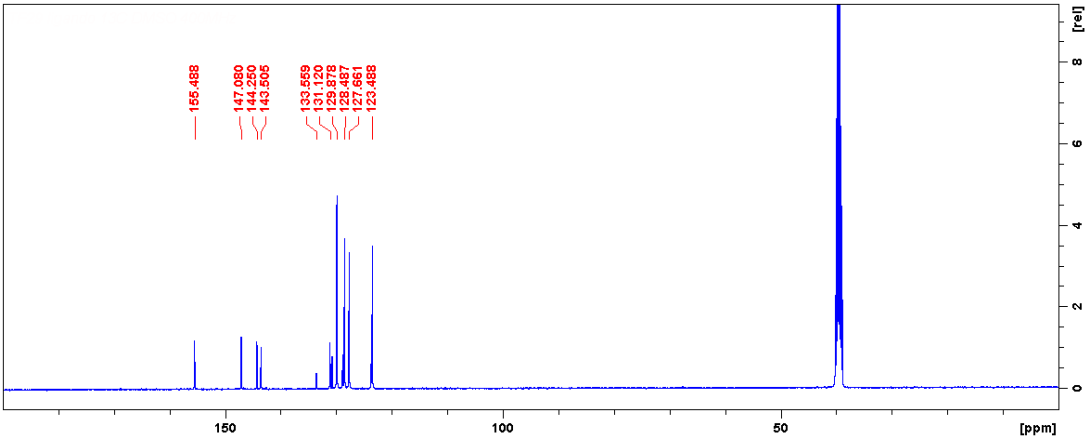

Figure S8. ^{13}C NMR spectrum of compound **1** (DMSO-d_6, 100 MHz).

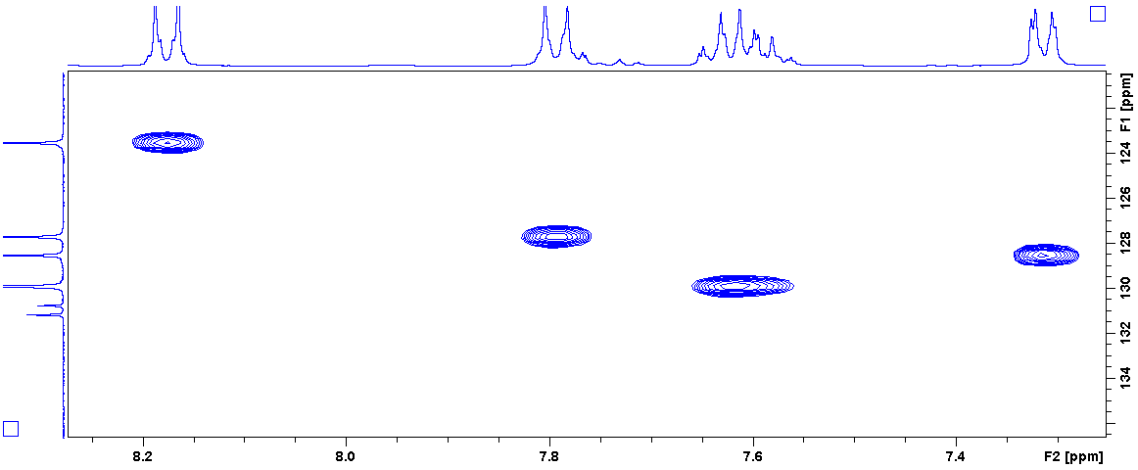

Figure S9. HSQC NMR spectrum of compound **1** (DMSO-d_6).

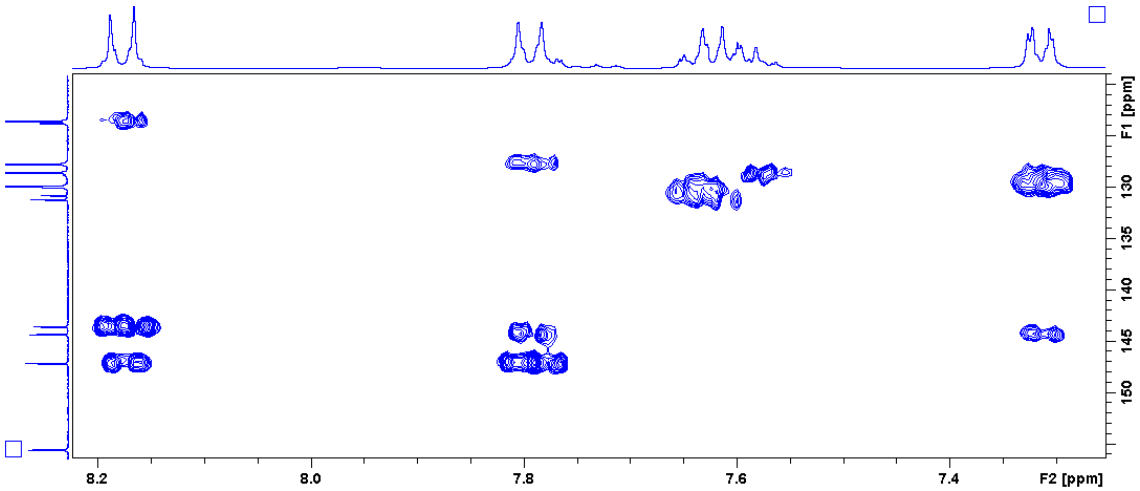

Figure S10. HMBC NMR spectrum of compound **1** (DMSO-d_6).

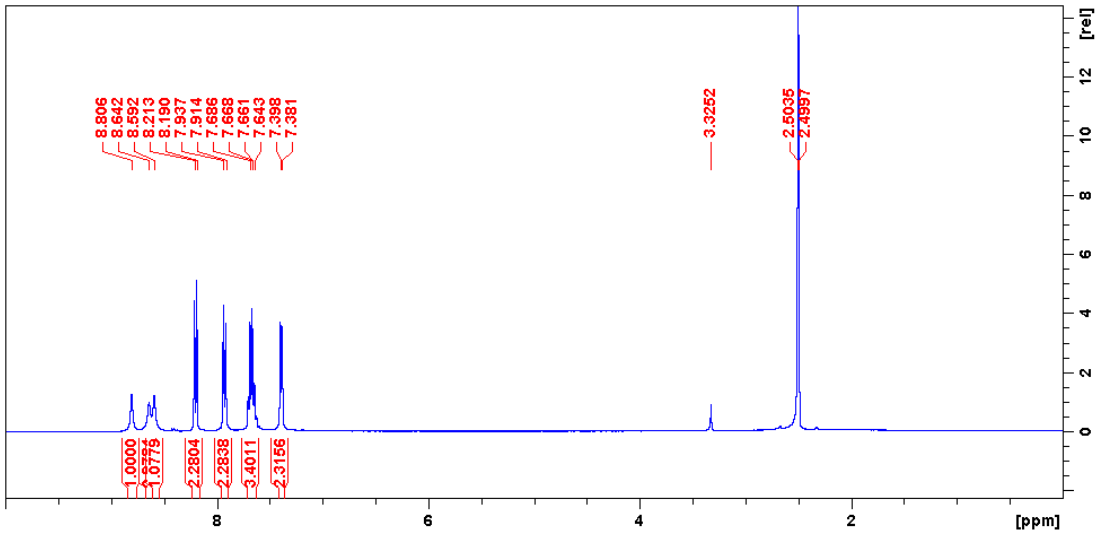

Figure S11. ^{1}H NMR spectrum of compound **2** (DMSO-d_6, 400 MHz).

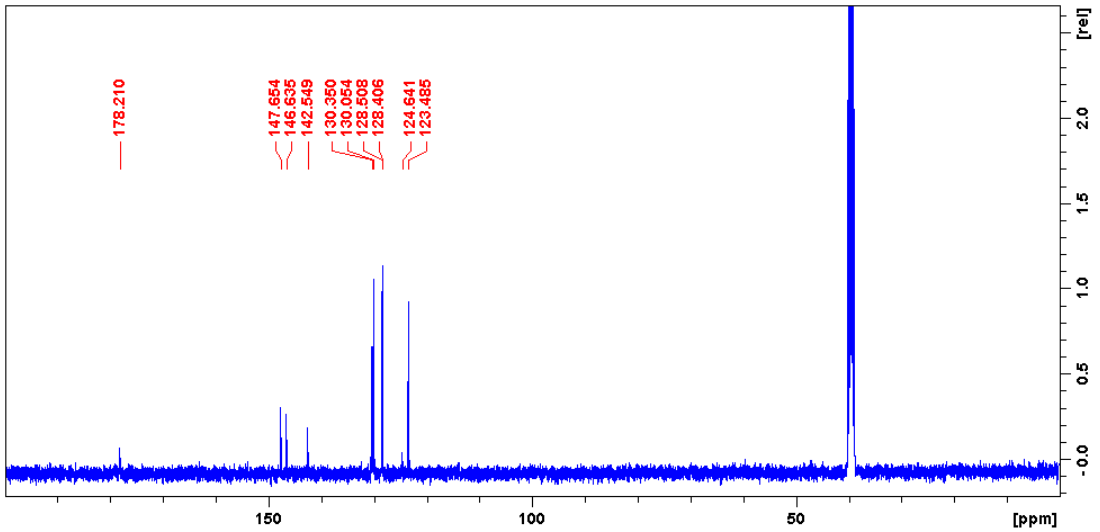

Figure S12. ^{13}C NMR spectrum of compound **2** (DMSO-d_6, 100 MHz).

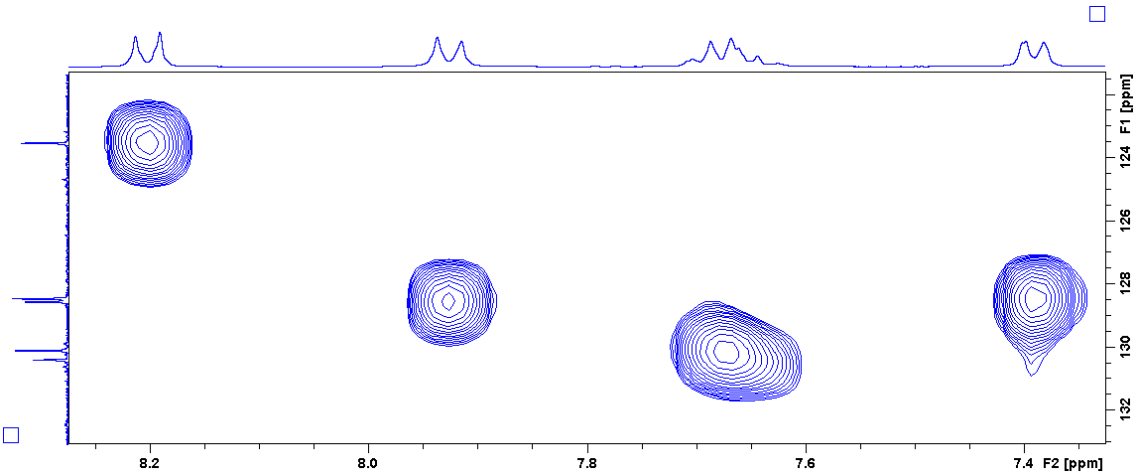

Figure S13. HSQC NMR spectrum of compound **2** (DMSO-d_6).

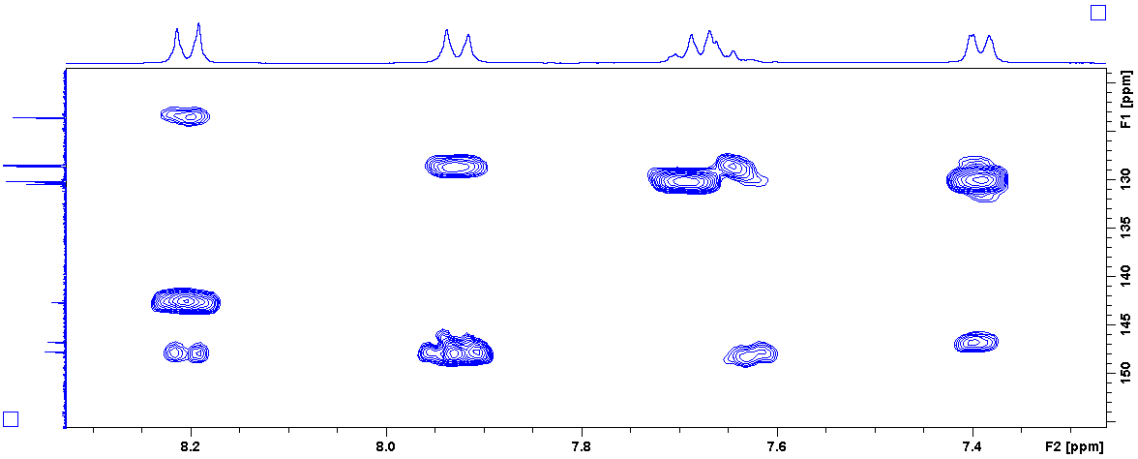

Figure S14. HMBC NMR spectrum of compound **2** (DMSO-d_6).

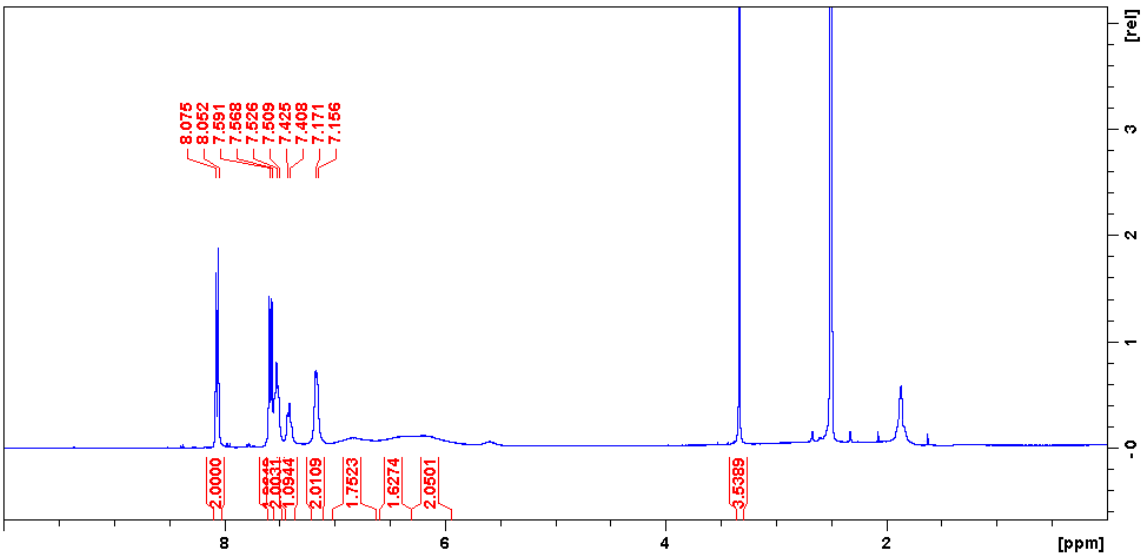

Figure S15. ^{1}H NMR spectrum of compound **3** (DMSO-d_6, 400 MHz).

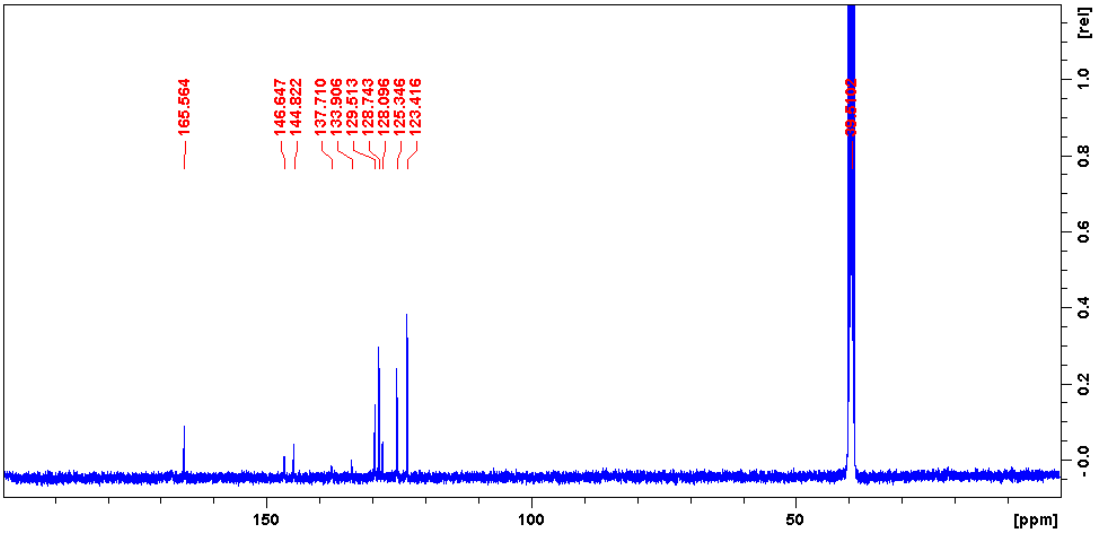

Figure S16. ^{13}C NMR spectrum of compound **3** (DMSO-d_6, 100 MHz).

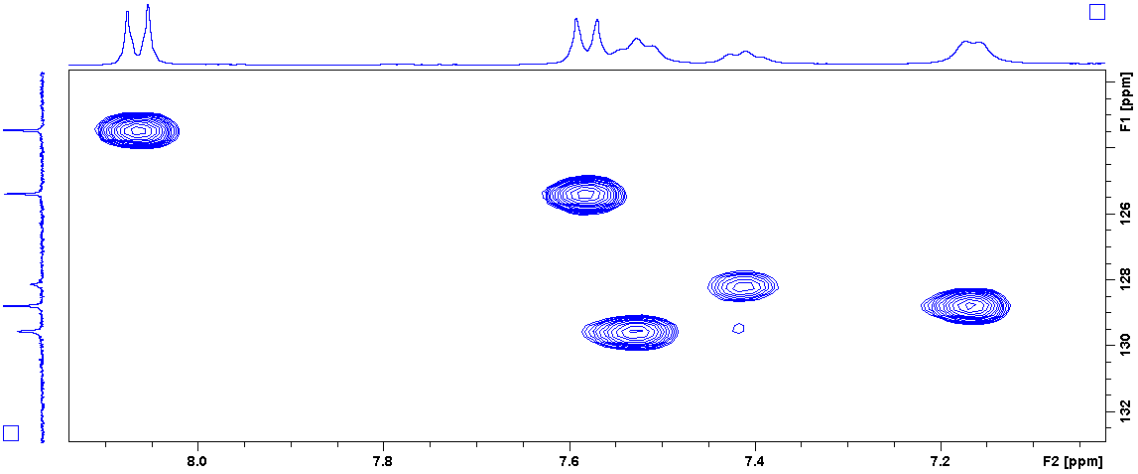

Figure S17. HSQC NMR spectrum of compound **3** (DMSO-d_6).

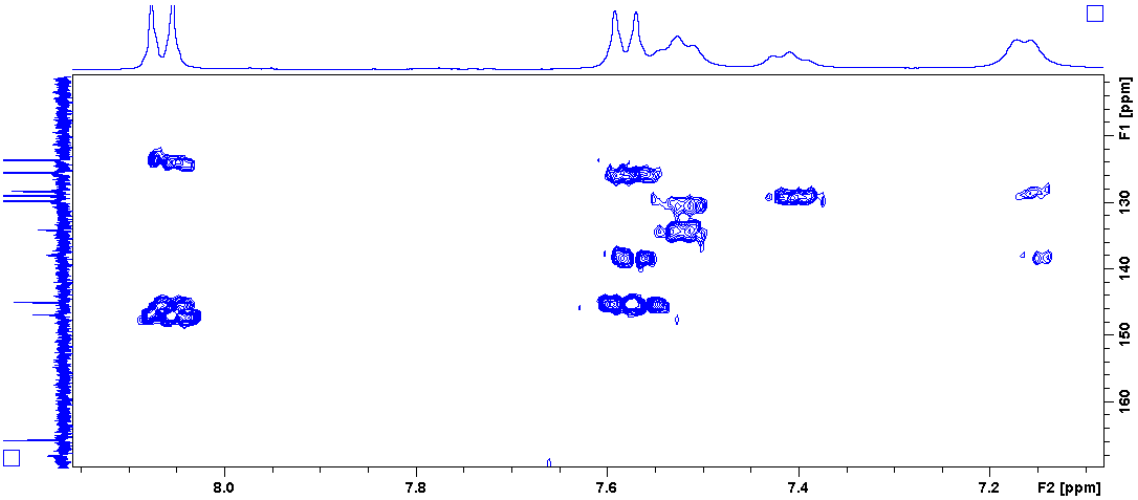

Figure S18. HMBC NMR spectrum of compound **3** (DMSO-d_6).

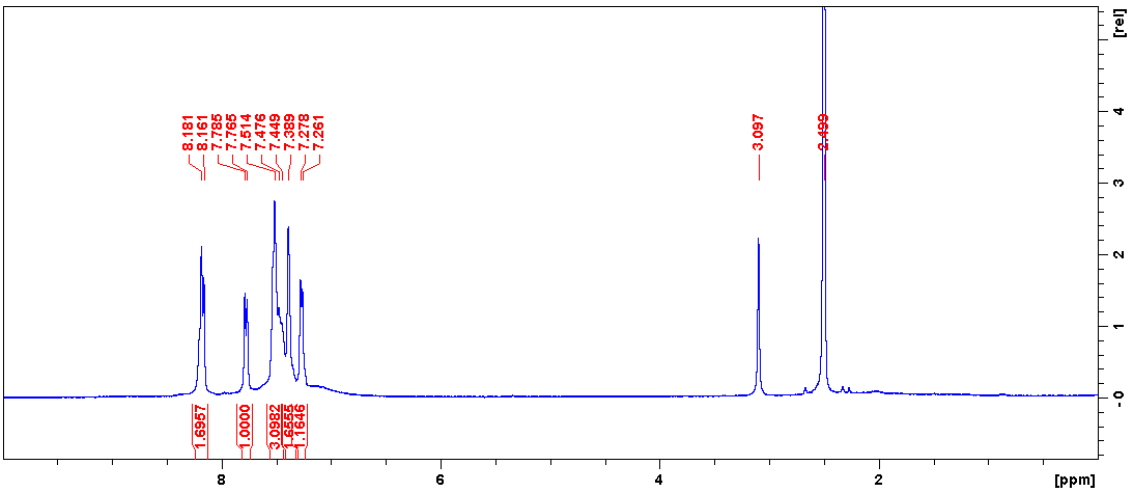

Figure S19. ^{1}H NMR spectrum of compound **4** (DMSO-d_6, 400 MHz, at 70 ºC).

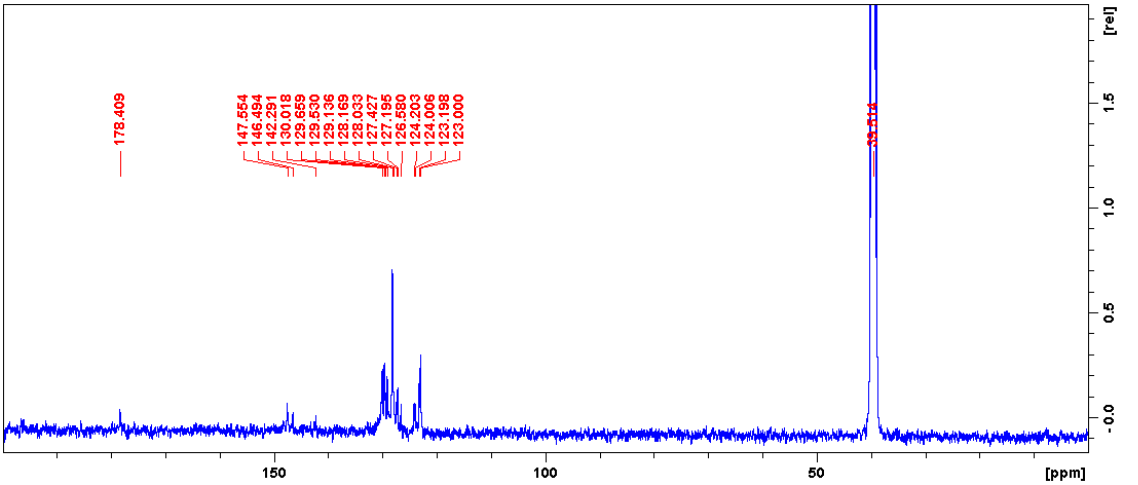

Figure S20. ^{13}C NMR spectrum of compound **4** (DMSO-d_6, 100 MHz, at 70 ºC).

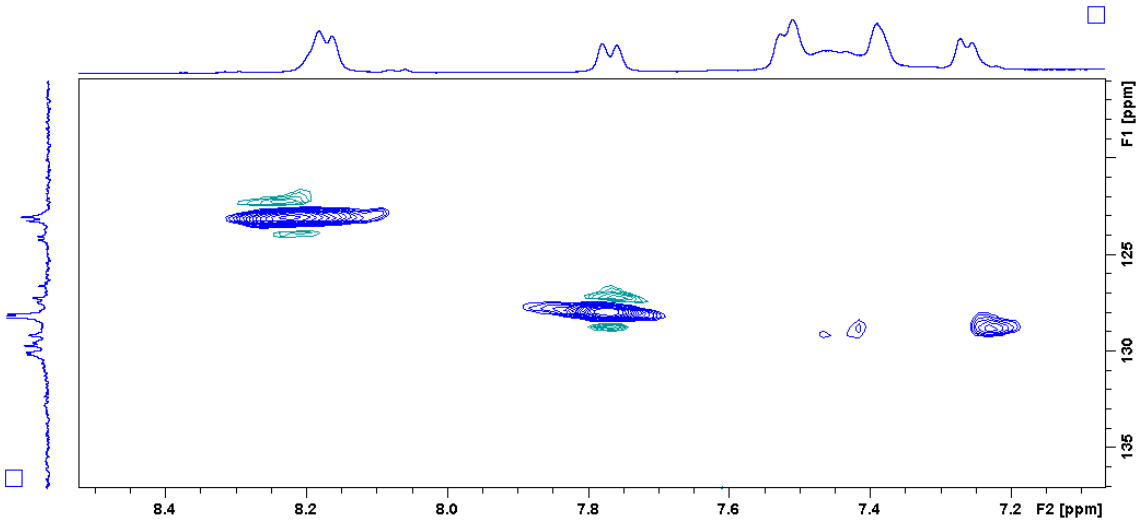

Figure S21. HSQC NMR spectrum of compound **4** (DMSO-d_6, at 70 ºC).

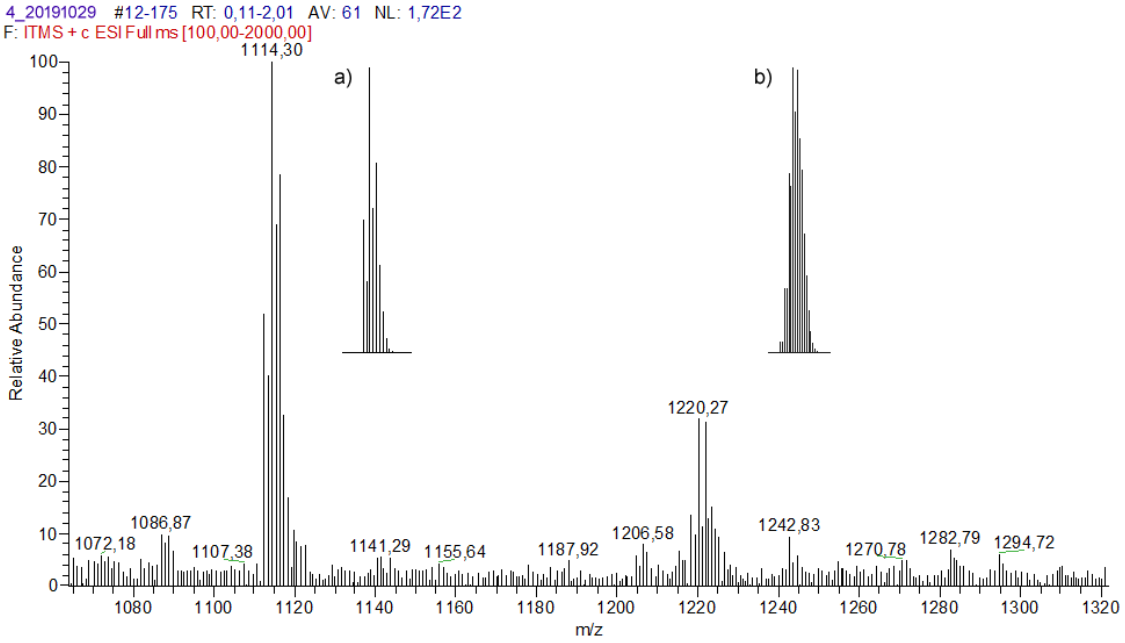

Figure S22. ESI-MS(+) spectrum of the Ag_6 complex **4** with experimental and predicted (insets a and b) isotopic distribution[S6] for (a) $[Ag_2(L^2)_3 + H]^{+\cdot}$ (m/z = 1114) and (b) $[Ag_6(L^2)_6 + H]^{2+\cdot}$ (m/z = 1221).

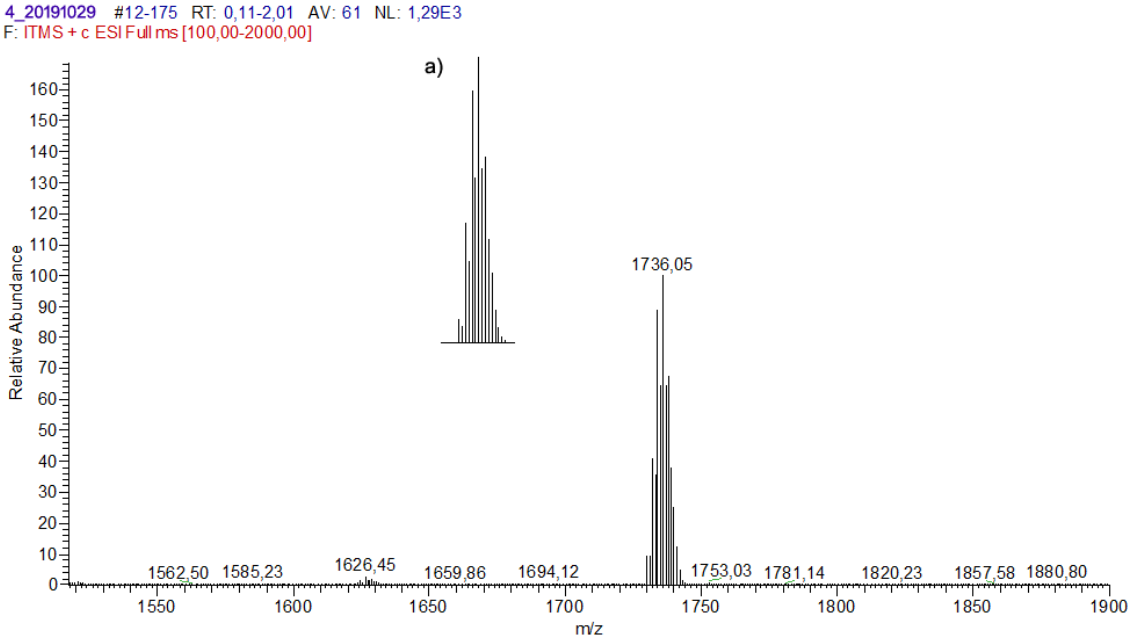

Figure S23. ESI-MS(+) spectrum of the Ag_6 complex **4** with experimental and predicted (inset a) isotopic distribution[S6] for $[Ag_5(L^2)_4]^+$ (m/z = 1735).